WIRELESS COMMUNICATIONS AND MOBILE COMPUTING
Wirel. Commun. Mob. Comput. 2016; **16**:1510–1525
Published online 20 July 2015 in Wiley Online Library (wileyonlinelibrary.com). DOI: 10.1002/wcm.2613

RESEARCH ARTICLE

Optimizing the throughput-lifetime tradeoff in wireless sensor networks with link scheduling, rate adaptation, and power control

Mejdi Kaddour*

LITIO Laboratory, Department of Computer Science, University of Oran 1, BP 1524 El-M'Naouer, Oran 31000, Algeria

ABSTRACT

Throughput and lifetime are usually conflicting objectives in designing wireless sensor networks; hence, the right balance needs to be found. With this aim in view, we address in this paper the problem of minimizing the frame length defined within a time division multiple access scheme and the problem of maximizing network lifetime subject to a maximum frame length. The pursued solution in either case leverages a wide range of parameters related to coverage, routing, transmission power, and data rate. Furthermore, it is consistent with the physical interference model. To this end, we rely on column generation technique to derive near-optimal solutions even when the integrality constraints on coverage and flow variables are enforced. Moreover, we propose a polynomial-time heuristic algorithm to solve efficiently the underlying NP-hard problem of concurrent link selection with discrete power control and rate adaptation. Simulation results show that our heuristic algorithm leads to solutions within 3% of optimality while saving around 99% of computation time. Besides, the results illustrate the significant impact of power control and rate adaptation on throughput and lifetime improvement. Interestingly, we found that network lifetime can be significantly prolonged when traffic demands are sufficiently low at the affordable cost of small decrease in throughput.

KEYWORDS
WSNs; TDMA; link scheduling; power control; SINR; column generation

***Correspondence**
Mejdi Kaddour, LITIO Laboratory, Department of Computer Science, University of Oran 1, BP 1524 El-M'Naouer, Oran 31000, Algeria.
E-mail: kaddour.mejdi@univ-oran.dz

1. INTRODUCTION

Although most of the state-of-the-art wireless sensor networks (WSNs) are formed by nodes that are designed to operate in an autonomous and distributed fashion, some recent works in the literature such as [1] or [2] indicate that centrally coordinated protocols at the network and the medium access control (MAC) layers are at least as efficient as distributed protocols in numerous settings while bringing other advantages such as code simplicity, ease of management, and observability. In particular, many WSN applications exhibit a regular traffic pattern by periodically collecting sensor measurements at a centralized entity known as the sink. In this context, time division multiple access (TDMA) offers a convenient access scheme at the MAC layer because it guarantees high bandwidth utilization and low energy consumption. In TDMA, the time is divided into frames each containing a certain number of fixed size slots. Typically, a central entity is responsible to define a frame schedule, assigning each node a fixed number of slots for transmitting and receiving data. Moreover, several transmission links could be scheduled in the same slot if no harmful level of interference occurs between them. To a great extent, interference is captured in theoretical studies or simulation using the protocol interference model and the physical model. Under the protocol model, a successful transmission occurs when the intended receiving node falls inside the transmission range of its transmitting node and falls outside the interference ranges of other non-intended transmitters. On the other hand, under the physical model, a transmission is successful if and only if the *signal-to-interference-and-noise ratio* (SINR) at the intended receiver exceeds a certain threshold so that the transmitted signal can be decoded with an acceptable bit error rate. This model is widely considered as a more accurate representation of the behavior of real systems [3].

More generally, regardless of a specific paradigm or technology for multihop wireless networks, throughput and lifetime could be intuitively considered as conflicting

objectives. For example, selecting short paths with high bandwidth and link quality is requested to achieve high throughput, in particular when the traffic is destined to few designated nodes such as a sink in a WSN. But that frequently implies that some limited-energy nodes have to carry a heavy burden by relaying large volume of traffic, may be using high transmission power, hence reducing their lifetime drastically. Conversely, a potential way to increase network lifetime would be to distribute the traffic evenly over more disjoint paths, so that more nodes are involved in relaying. However, this may decrease the overall throughput and even increase unfairness because of longer paths or poor radio conditions on some links. Hence, a nontrivial tradeoff between these two objectives has to be determined depending on user requirements, application type, network topology, or traffic pattern.

In this paper, we are motivated to investigate the achievable performance and also the tradeoffs that arise in TDMA WSNs using cross-layer optimization models that encompass coverage, quality of service, and lifetime requirements. In particular, we focus on surveillance WSNs where a set of targets must be continuously monitored by a set of sensors with limited amount of energy. One of the main challenges in designing TDMA for multihop wireless networks, in general, is to derive a link schedule optimizing user-defined performance metrics such as throughput, end-to-end delay, energy consumption, or fairness index. Typically, one common goal of optimization models is to minimize the number of slots per frame as it implies maximizing capacity. The key issue here is how to mitigate interference by adapting transmit powers, traffic routes, or channel bandwidth to the network topology and the traffic requirements. We address two closely related problems: (i) determine a minimum length TDMA schedule to maximize network throughput and (ii) maximize network lifetime subject to a maximum schedule length. In both problems, we consider an SINR-based interference model. The sought solution is to determine the routes, the sensors that generate traffic, the transmission powers, and the data rate on each link, in a way to optimize the objective function.

The adopted approach, formulated initially as an integer linear program (ILP), relies on column generation (CG) technique to decouple traffic and bandwidth management from feasible matching generation. We refer throughout this paper to a feasible matching as a set of transmission links with associated data rates that can be scheduled concurrently, in order to improve the spatial reuse. Due to its high complexity, this underlying subproblem is otherwise tackled by a computationally efficient heuristic algorithm, based on the necessary and sufficient conditions for which several links with variable powers can be scheduled simultaneously, as well as a supporting conflict graph. Other features of our contribution are summarized as follows:

(1) In most works, authors assume that the power level can be adjusted to the exact needs and calculate the SINR and the energy consumption using continuous values. In contrast, our model relies on a finite set of discrete power levels as it is the case in real-world radio transceivers.
(2) Each sensor is able to encode and modulate the radio signal to transmit with different data rates.
(3) Most papers assume known traffic demands at each sensor node. Our model rather returns as a result the amount of traffic originating from each sensor by determining which sensors cover each target.
(4) We consider the so-called Q-coverage requirement, where a target can be associated to multiple sensors providing redundancy and reliability to measurements.
(5) The considered energy model is based on transmit and receive power dissipations observed in a real-world platform. Besides, the energy consumed for target monitoring is reasonably assumed to be linearly dependent on the distance between the sensor and the target.

The rest of this paper is organized as follows. We discuss related work in Section 2. Section 3 introduces the network model as well as the assumptions used throughout this paper. We expose in Section 4 our column-generation-based model to maximize network throughput. This is followed in Section 5 by a description of the optimization model designed for the lifetime maximization problem. Section 6 is devoted to a detailed presentation of our heuristic approach to solve the subproblem of finding an enhancing feasible matching. Section 7 discusses the results of various experiments illustrating the computational performance of our approach, the effects of node density and coverage level on the throughput, and highlighting the throughput-lifetime tradeoffs. Finally, conclusions are drawn in Section 8.

2. RELATED WORK

The problem of scheduling concurrent transmission links by satisfying the SINR requirement at each link in TDMA wireless networks has been extensively studied in the literature. In [4], the authors solved the problem via two alternating phases that define a set of admissible links along with their transmission power. The main contribution was to eliminate the need of computationally expensive algorithms by splitting the problem and executing the power control in a distributed fashion. However, the general problem of determining a minimum-length schedule that satisfies given traffic demands and subject to SINR constraints is NP-hard as shown in [5]. Many polynomial-time approximation algorithms were proposed on this issue. The authors in [6] studied joint link scheduling and power control with the objective of throughput improvement while considering fairness through a new introduced factor called *demand satisfaction*. After the original model was formulated as a mixed-integer linear program (MILP), the key idea was to use the solutions obtained from a serial linear programming relaxed version of the problem as guidelines

to schedule the radio channel. In [7], the authors addressed the problem through a heuristic algorithm called *increasing demand greedy scheduling* (IDGS). This algorithm defines a set of feasible matchings by considering link demands in the increasing order. IDGS is further improved through a CG-based method. Furthermore, inspired by the work of Grandhi *et al.* [8], the Perron–Frobenius eigenvalue condition, which determines the feasibility of a given matching, is used as a tie to solve link scheduling and power control in an integrated manner. Recently, the authors in [9] proposed a scheduling algorithm of transmission links together with source rate control as a small-timescale approach, which exploits receiver diversity when receivers of multiflows can have different channel conditions because of varying interference.

Time division multiple access scheduling may introduce large delays in multihop wireless networks. An optimization model is formulated in [10] with the aim to find a transmission schedule with the min–max delay. In the particular case of overlay tree topologies, a polynomial time algorithm based on Bellman–Ford shortest path is devised. However, the authors rely only on pairwise conflict graphs that ignore the cumulative effect of interference. In [11], the authors considered the problem of assigning time slots to different users to minimize channel usage subject to constraints on data rate, delay bound, and delay bound violation probability, under a SINR-based interference model. Besides, the minimum-length scheduling problem with power control subject to traffic demands and SINR constraints was addressed in [12]. The adopted approach is to separate link demand satisfaction from feasible matching generation through CG. The feasible matching problem that has no known polynomial-time algorithm was simplified by using the Perron–Frobenius condition and a so-called smart enumerating algorithm that has exponential runtime. A graph coloring-based approach was proposed in [13] to solve the TDMA scheduling in the context of WSNs where data are transferred to few data collectors. In [14], the authors introduced a *power-controlled rate adaptation interference graph* as a means to minimize the TDMA schedule length assuming adaptive power and link rate. The solution is derived through a greedy algorithm constructing an independence set from this graph. Another example of CG application considering SINR constraints is given in [15]. The proposed model considers joint routing and schedule minimization with variable transmit powers and data rates. A lower bound on the solution is updated at each iteration of the master problem to terminate the procedure once a user-specified optimality gap is attained. The authors in [16] considered convergence cast latency in wireless sensor/actuator networks. The minimization of this latency is achieved first by minimizing the separation distance of concurrent data transmissions, so that the number of nodes sending data in the same time slot is maximized. They examined the relationship between the hop separation, the SINR, and the latency to make a selection of interference separation.

On the other hand, many optimization techniques have been used over the past few years to maximize the lifetime of WSNs. In [17], the authors considered the optimization of individual layers as well as cross-layer optimization in TDMA WSNs. A convex optimization model is defined to maximize network lifetime as a function of routing, transmission powers, and link scheduling. For particular cases of linear and single-source single-sink planar topologies, Karush–Kuhn–Tucker optimality conditions are used in [18] to derive analytical expressions of optimal network lifetime. Whereas, in more general planar configurations, suboptimal solutions are computed by using a decomposition and combination approach. Other works focused on target coverage problem [19], which states that each target needs to be monitored by at least one sensor at any time while maximizing lifetime. The problem was formulated in a nonlinear form in [20], but two lifetime upper bounds are obtained via linear relaxation techniques. The authors in [21] further extended the problem by assuming multiple-target coverage that would make the amount of collected data varies between sensors. A more challenging version was proposed in [22], where a MILP is designed to maximize lifetime while determining sensor locations, routing, and activity schedules. Sensors with adjustable sensing ranges were considered in [23], where a genetic algorithm was formulated to build coverage sets. The main idea was to save energy by associating targets with the closest sensors.

Still that few works have considered the interplay between throughput and lifetime in WSNs. In [24], the authors proposed a weighted linear combination of lifetime and rate allocation to characterize this tradeoff in their optimization models. Considering that the minimum frame length TDMA link scheduling problem has multiple optimal solutions, the work in [25] addressed the issue of jointly minimizing power consumption and maximizing quality of service through a lexicographic framework and local search. The work in [26] is among the most closest to us, as it addressed a set of problems in WSNs where lifetime is maximized while achieving a required max–min throughput, and vice-versa. However, the authors were mainly committed to derive analytical results characterizing the tradeoffs between optimal throughput (or lifetime) versus lifetime (or throughput) and transmit power. In this paper, our objective is rather to provide a method able to compute efficiently near-optimal solutions of realistic network instances. Moreover, to the best of our knowledge, no prior work has considered both optimizing TDMA schedule and target coverage in WSNs subject to throughput constraints by leveraging such a wide set of network parameters.

3. NETWORK MODEL

We consider a set of n sensors, denoted as $S = \{s_1, s_2, \ldots, s_n\}$ and a set of h targets, denoted as $T = \{t_1, t_2, \ldots, t_h\}$, deployed arbitrary on a given area. Each target must be covered by q sensors (Q-coverage). We assume

that a target can be covered by a given sensor if the Euclidean distance between them does not exceed the sensing range R_{max}. Each sensor generates a data packet of size σ bits each time it monitors an associated target. All monitored data must be communicated, possibly after passing through several hops, to a sink node, labeled as s_0.

We assume that each sensor is equipped with a single radio that can be tuned dynamically without a significant delay to transmit according to one of K discrete power levels $P_1 < P_2 < \cdots < P_K$. Traffic flows inside the network can be represented by a directed graph $G = \{S \cup \{s_0\}, E\}$ with $E = \{(s_i, s_j) \mid i = 1, \ldots, n,\ j = 0, \ldots, n\}$. There exists an arc from s_i ($i \neq 0$) to s_j if the separating distance d_{ij} is less than the transmission range produced by P_K. According to a given deployment of sensors and targets on the area, we assume that all sensors have a valid path toward the sink. Furthermore, sensors are assumed to be able to transmit according to R modulation and coding schemes (MCSs). Each MCS_r ($1 \leq r \leq R$) produces a certain date rate θ_r ($\theta_1 < \theta_2 < \ldots < \theta_R$). A transmission with rate θ_r could be decoded successfully is the signal-to-noise ratio (SNR) measured at the receiver is above a corresponding threshold β_r. Clearly, the higher data rate is employed; the higher SNR is required.

According to the physical model [27], a direct transmission link ℓ could be established between two different nodes, that is, $\ell \in E$, if the following condition holds:

$$G_\ell \geq \frac{\beta_1 N_0}{P_K} \tag{1}$$

where G_ℓ denotes the propagation gain between the transmitter and the receiver and N_0 is the thermal noise power.

In presence of interference caused by concurrent links $\ell' \in E$, a transmission link ℓ with data rate b_k would be successful if SINR_ℓ measured at the intended receiver is greater than or equal to β_k. It is given by

$$\text{SINR}_\ell = \frac{p_\ell G_\ell}{N_0 + \sum\limits_{\ell\prime \in E \setminus \{\ell\}} p_{\ell\prime} G_{\ell\prime\ell}} \tag{2}$$

where p_ℓ is the transmission power of ℓ and $G_{\ell\prime\ell}$ denotes the propagation gain between the transmitter of $\ell\prime$ and the receiver of ℓ.

In addition, we assume a TDMA access scheme, where a central entity divides the time cyclically into slots of fixed duration, which are then grouped into frames. The duration of each slot is T_s, which corresponds to the time required to send a data packet of σ bits using the lowest data rate θ_1. A TDMA schedule defines the group of admitted transmission links within each time slot so that the SINR at each receiver is above the corresponding required threshold. We neglect voluntarily the slots that might be needed for control and synchronization purposes as their number is generally constant. Also, we assume that each sensor generates one data packet for each monitored target during the TDMA frame. Hence, all the targets receive equal treatment by the network. Finally, all data packets have to be collected by the sink by the end of the TDMA frame.

4. THROUGHPUT MAXIMIZATION PROBLEM

The throughput of a WSN is measured in this paper by the overall traffic that reaches the sink per time unit. The throughput-delay relationship is straightforward to derive because the end-to-end delay between a sensor and the sink is bounded by the TDMA frame length, which in turn determines the throughput. However, as more targets are monitored inside the network, the TDMA frame length would increase, implying potential larger delays, while the total throughput would remain stable. Hence, transmission ordering becomes critical in this case, but we are here primarily interested in optimizing the overall throughput, so the end-to-end delay is not explicitly considered.

Our objective is to define a minimum-length TDMA schedule by determining jointly which sensors cover each target, the scheduled concurrent links at each slot, along with their used MCSs and power levels, and the established routes toward the sink. We refer to this problem in the rest of the paper as TMP.

A straightforward optimization model for the TMP problem consists in introducing a binary decision variable $x_{\ell rt}$ which indicates if the link ℓ with data rate θ_r is active during the slot t. The major drawback with this formulation is the huge number of required binary variables: $|E| \times R \times T_{max}$. Because the length of the TDMA frame is also a decision variable, the parameter T_{max}, denoting the maximal number of slots in a frame, should be chosen large enough to hold the resulting transmission schedule. Otherwise, the problem will be infeasible.

Alternatively, in the same manner as [15] or [28], our model is based on the notion of *matching* (or *configuration*) that represents a set of transmission links that can be scheduled concurrently without violating the SINR requirement at each receiver. Despite the exponential number of feasible matchings, which scales up following the cardinality of the power set of E ($2^{|E|}$), we need in fact only a small subset of those matchings to resolve the problem as we will see in the following.

A matching m is formally defined in this paper as

$$m = \left\{ \left(x^m_{\ell r}, p^m_{\ell k}\right) \mid \ell \in E,\ r = 1, \ldots, R,\ k = 1, \ldots, K, \right. \\ \left. SINR_\ell \geq \beta_r,\ \sum_{r=1}^{R} x_{\ell r} \leq 1,\ \sum_{k=1}^{K} p_{\ell k} \leq 1 \right\} \tag{3}$$

where $x^m_{\ell r}$ and $p^m_{\ell k}$ are binary parameters indicating if the link ℓ is scheduled in m using data rate r and power level index k, respectively. The set of all feasible matchings is denoted as $\mathcal{M}$.

Let the integer decision variable λ_m refers to the number of slots in which the matching m is scheduled. Let y_{ij} be a binary variable indicating if the target t_j is covered by the sensor s_i ($i \neq 0$). In addition, let f_ℓ be an integer variable counting the number of data packets transmitted on the link ℓ during the whole TDMA frame. The transmitter and the receiver of a link ℓ are referred to as $t(\ell)$ and $r(\ell)$, respectively. The TMP problem can be formulated by the following ILP:

$$\text{[TMP] minimize} \sum_{m \in \mathcal{M}} \lambda_m \tag{4}$$

subject to:

$$\sum_{s_i \in S} y_{ij} = q \qquad t_j \in T \tag{5}$$

$$\sum_{\substack{\ell \in E \\ r(\ell)=s_i}} f_\ell + \sum_{t_j \in T} y_{ij} = \sum_{\substack{\ell \in E \\ t(\ell)=s_i}} f_\ell \qquad s_i \in S \tag{6}$$

$$\sum_{\substack{\ell \in E \\ r(\ell)=s_0}} f_\ell = hq \tag{7}$$

$$\sum_{m \in \mathcal{M}} \sum_{r=1}^{R} \theta_r T_s x_{\ell r}^m \lambda_m - f_\ell \sigma \geq 0 \qquad \ell \in E \tag{8}$$

$$\lambda_m \geq 0 \text{ and integer}, \qquad m \in \mathcal{M} \tag{9}$$

$$f_\ell \geq 0 \text{ and integer}, \qquad \ell \in E \tag{10}$$

$$y_{ij} \in \{0, 1\}, \qquad s_i \in S, t_j \in T \tag{11}$$

Constraint (5) ensures that every target is covered by exactly q sensors. Constraint (6) represents flow conservation rule by stating that the amount of incoming traffic into a sensor, which is made up by traffic forwarded by other sensors and the traffic generated locally by monitoring associated targets, is equal to the amount of outcoming traffic. Constraint (7) guarantees that all data packets are gathered by the sink. The channel capacity constraint (8) ensures that the number of times link ℓ is included in all the scheduled matchings ($\lambda_m > 0$) is sufficient to forward the assigned traffic.

Note that this matching-based ILP model does not provide a transmission ordering of the matchings as the straightforward model does. Nevertheless, this has no impact on the total throughput because the matchings can be scheduled at any order within the frame without changing its length. Now, this model is solvable if we can determine by some means the set $\mathcal{M}$. But enumerating all feasible matchings would be computationally very expensive. We present in the next subsection a technique to alleviate this issue.

4.1. Column generation approach

Column generation is an exact and efficient algorithm for solving large-scale linear programs. The main idea relies on the fact that most of the variables will be non-basic (equal to zero) in the optimal solution. Hence, only a subset of variables (or columns) needs to be considered in theory when solving the problem. The problem being solved is split into two subproblems: *the restricted master problem* (RMP) and the *the pricing problem*. The RMP is the original problem with only a subset of variables being considered. The pricing problem is another problem created to generate only the variables that have the potential to improve the objective function, that is, to find variables with negative reduced costs in case of a minimization problem. The algorithm alternates then between these two subproblems until no variable that would enhance the objective function is found.

In our case, the RMP is formulated as in (4)–(8) but considers only a subset $\mathcal{M}_0$ of feasible matchings $\mathcal{M}$. As CG is a linear programming technique, we need also to make a linear relaxation on the integer variables λ_m, f_ℓ, and y_{ij}. On the other hand, the pricing problem relies on finding a new feasible matching with a minimum reduced cost. Let u_ℓ be the dual variables associated with (8); the reduced cost of any matching m not currently in $\mathcal{M}_0$ can be written as

$$e_m = 1 - \sum_{\ell \in E} \sum_{r=1}^{R} u_\ell \theta_r T_s x_{\ell r}^m \tag{12}$$

If the minimum reduced cost has a strictly negative value, the corresponding matching (column) is added to $\mathcal{M}_0$, and the RMP is solved again; otherwise, the optimal solution has been reached.

The pricing problem can be stated as follows:

$$\text{[TMP-Pricing] Minimize}_{m \in \mathcal{M}} \; e_m \tag{13}$$

subject to

$$\sum_{\substack{\ell \in E \\ s_i \in \{t(\ell), r(\ell)\}}} \sum_{r=1}^{R} x_{\ell r} \leq 1 \qquad s_i \in S \tag{14}$$

$$\sum_{k=1}^{K} p_{\ell k} \leq 1 \qquad \ell \in E \tag{15}$$

$$\sum_{k=1}^{K} G_\ell P_k p_{\ell k} - \beta_r \left(\sum_{\ell' \in E \setminus \{\ell\}} \sum_{k=1}^{K} G_{\ell' \ell} P_k p_{\ell' k} + N_0 \right) \geq L_1 (x_{\ell r} - 1) \qquad \ell \in E, 1 \leq r \leq R \tag{16}$$

$$x_{\ell r} \in \{0, 1\} \qquad \ell \in E, \; 1 \leq r \leq R \tag{17}$$

$$p_{\ell k} \in \{0, 1\} \qquad \ell \in E, \; 1 \leq k \leq K \tag{18}$$

where L_1 is a sufficiently large positive constant. Constraint (14) states that a node cannot transmit and receive at the same time and only one data rate is active. Constraint (15) forces a transmitter to select only one power level. Constraint (16) is an enforcement of rule (2) by ensuring that the SINR at the receiver must be above the threshold β_r when the variable $x_{\ell r}$ is nonzero. Otherwise, this constraint is redundant.

The CG technique requires an initial basic feasible solution to be provided to the RMP, that is, a set of matchings $\mathcal{M}_0$ that leads to an initial solution verifying flow, channel capacity, and coverage constraints. This solution is obtained by applying the minimum spanning tree algorithm [29] to an undirected graph equivalent to G, where each edge gets the same weight. Then, every edge of the resulting tree is included in a new matching by setting the corresponding transmission link in the direction of the sink and with the highest rate that it can achieve. The obtained $\mathcal{M}_0$ guarantees a feasible solution because each sensor node is the transmitter of some link ℓ that is included in exactly one matching in $\mathcal{M}_0$. Any amount of outcoming flow at this node can be transmitted by scheduling ℓ as many times as necessary to satisfy constraint (8). The remaining constraints in the TMP (5)–(7) represent flow conservation and do not involve $\mathcal{M}_0$.

4.2. Near-optimal solution of the TMP problem

The CG technique solves a linear relaxed version of the original ILP problem, but a more effective solution to the problem would be to determine an integer number of slots, and integer coverage and flow variables. Actually, the coverage variables y_{ij} indicate whether or not a target is covered by a given sensor (0 or 1), and the flow variables f_ℓ specify the number of data packets transmitted on the link ℓ during the TDMA frame. Clearly, a data packet should reach the sink as a whole entity without a costly fragmentation.

Consequently, we propose here a heuristic to figure out a near-optimal solution of the ILP. Let Z^{LP} and Z^{ILP} denote the optimal solutions of the problem, considering continuous and integer RMP variables, respectively. Let Z^* be the solution obtained by solving the ILP version of the RMP after all the columns with negative reduced costs have been added and consequently Z^{LP} has been obtained. It is clear that $Z^{LP} \leq Z^{ILP} \leq Z^*$. So the optimal integer solution lies somewhere between Z^{LP} and Z^*. As shown in Section 7, this interval is found to be very small and in most cases does not even hold an integer other than Z^*.

5. LIFETIME MAXIMIZATION PROBLEM

We develop in this section a MILP formulation of the problem of maximizing the network lifetime subject to a given TDMA frame length. The network lifetime is defined here as the time elapsed from the starting of network operation to the moment when a first sensor runs out its energy. The sensor's total energy consumption is composed from sensing energy and radio transmission energy. We denote by e^s_{ij} the energy consumed by sensor s_i each time it monitors target t_j. Similarly to [19] and [23], we assume that sensing energy is a linear function of the distance between the sensor and the target. That is,

$$e^s_{ij} = e^s_{max} \frac{d_{ij}}{R_{max}} \tag{19}$$

where e^s_{max} is the amount of energy dissipated in sensing a target at distance R_{max}.

Besides, the energy consumed by the radio module depends on its operational state: transmit, receive, and idle. In each case, it is given by the product of the required power level and the time spent in that state. Specifically, based on CC2420 radio transceiver specifications [30], the output power in each state is calculated as the product of the current drawn and the supply voltage. The current drawn in idle state is generally negligible compared to other states; hence, we do not consider it in our model. Note also that sensors are spared from consuming energy in idle listening as channel access is deterministic with TDMA.

Denoting by P^{tx}_k the power consumed by a sensor in transmit state when using transmission power level P_k ($1 \leq k \leq K$) and by P^{rx} the power consumed in receive state, the energy consumed by a sensor s_i during a TDMA frame can be written as

$$\begin{aligned} e_i = {} & \frac{e^s_{max}}{R_{max}} \sum_{t_j \in T} d_{ij} y_{ij} + \sum_{m \in \mathcal{M}} \sum_{\substack{\ell \in E \\ t(\ell) = s_i}} \sum_{k=1}^{K} \lambda_m T_s P^{tx}_k p^m_{\ell k} \\ & + \sum_{m \in \mathcal{M}} \sum_{\substack{\ell \in E \\ r(\ell) = s_i}} \sum_{r=1}^{R} \lambda_m T_s P^{rx} x^m_{\ell r} \end{aligned} \tag{20}$$

Maximizing the network lifetime implies minimizing the maximum fraction ρ of initial energy a sensor consumes during a TDMA frame. Hence, by reusing the CG technique as in Section 4.1, the RMP for this problem can be formulated as follows:

$$\text{[Lifetime-RMP] Minimize } \rho \tag{21}$$

subject to

$$e_i \leq E_i \rho \qquad s_i \in S \tag{22}$$

$$\sum_{m \in \mathcal{M}_0} \lambda_m T_s \leq T_{frame} \tag{23}$$

$$\sum_{s_i \in S} y_{ij} = q \qquad t_j \in T \tag{24}$$

$$\sum_{\substack{\ell \in E \\ r(\ell) = s_i}} f_\ell + \sum_{t_j \in T} y_{ij} = \sum_{\substack{\ell \in E \\ t(\ell) = s_i}} f_\ell \qquad s_i \in S \tag{25}$$

$$\sum_{\substack{\ell \in E \\ r(\ell)=s_0}} f_\ell = hq \tag{26}$$

$$\sum_{m \in \mathcal{M}} \sum_{r=1}^{R} T_s \theta_r x_{\ell r}^m \lambda_m - f_\ell \sigma \geq 0 \qquad \ell \in E \tag{27}$$

$$\lambda_m \geq 0 \qquad m \in \mathcal{M}_0 \tag{28}$$

$$f_\ell \geq 0 \qquad \ell \in E \tag{29}$$

$$y_{ij} \in [0,1] \qquad s_i \in S, t_j \in T \tag{30}$$

where E_i and T_{frame} are constants representing the initial energy of sensor s_i and the length of the TDMA frame, respectively. Note that because the computed TDMA frame length ($\sum_{m \in \mathcal{M}_0} \lambda_m T_s$) could be less than T_{frame} (23), the frame may contain an idle portion where no transmissions are scheduled. The remaining constraints are similar to those of the TMP problem.

The network lifetime in seconds can be expressed as the fraction T_{frame}/ρ. Sometimes, it would be preferable to express the lifetime as the number of achievable TDMA cycles, which corresponds to the total number of monitorings per target. In this case, it is simply given as $1/\rho$.

The associated pricing problem can be stated exactly as TMP-pricing except that the objective is replaced by

$$\begin{aligned} \text{Maximize } & \sum_{\ell \in E} \sum_{k=1}^{K} \frac{u_{t(\ell)} P_k^{tx}}{E_{t(\ell)}} p_{\ell k} \\ & + \sum_{\ell \in E} \sum_{r=1}^{R} \left(\frac{u_{r(\ell)} P^{rx}}{E_{r(\ell)}} + v_\ell \theta_r \right) x_{\ell r} + w \end{aligned} \tag{31}$$

where u_i ($1 \leq i \leq n$), v_ℓ ($\ell \in E$), and w are the dual variables of constraints (22), (23), and (27), respectively. A new matching would be added to the lifetime-RMP if the corresponding objective value is strictly greater than zero.

The lifetime-RMP requires an initial feasible solution consisting in a set of matching guaranteeing a TDMA schedule whose length is less than T_{frame}. This solution is provided by iterating between the TMP–RMP and the TMP-pricing by having the same instance as an input, but not further than the point where the objective corresponds to a frame length less than or equal to T_{frame}. Note that the final integer solution is obtained in the same manner as in Section 4.2.

6. A HEURISTIC-BASED APPROACH FOR THE PRICING PROBLEM

The TMP-pricing presented in Section 4 is a general form of the one-shot scheduling problem defined in [31]. The authors proved that the decision version of this problem is NP-complete by reduction from the Knapsack problem. We introduce in this section a polynomial-time algorithm to derive valid matchings by relying on schedulability conditions of concurrent links and a supporting conflict graph. Note that a valid matching is defined in the remainder as a feasible matching with $\sum_{\ell \in E} \sum_{r=1}^{R} u_\ell \theta_r T_s x_{\ell r}^m$ (as in (12)) greater than one. As a consequence of the NP-hardness of the problem, this algorithm may end up without finding a valid matching although a solution exists. In this case, the optimization process terminates with the current possibly non-optimal solution. Nevertheless, as illustrated in Section 7, the optimality gap is generally quite small.

6.1. Schedulability of concurrent links

In this section, a number of propositions found in [8], [12], and [32] are adapted to our problem. A matching m of z concurrent transmissions $(\ell_1, \gamma_1), (\ell_2, \gamma_2), \ldots, (\ell_z, \gamma_z)$, where ℓ_i denotes the link and γ_i denotes the associated data rate is scheduledable if and only if

(1) $t(\ell_i) \neq t(\ell_j), t(\ell_i) \neq r(\ell_j), r(\ell_i) \neq t(\ell_j)$, $r(\ell_i) \neq r(\ell_j)$, for $i \neq j$ and $i,j = 1, \ldots, z$

(2) $$\frac{P_{\ell_i} G_{\ell_i}}{N_0 + \sum\limits_{\substack{\ell_j \in m \\ \ell_j \neq \ell_i}} P_{\ell_j} G_{\ell_j \ell_i}} \geq \beta_i \quad \forall \ell_i \in m$$

where β_i is the minimal required SINR level to achieve data rate γ_i with an acceptable Bit Error Rate (BER). Putting $\psi_{ij} = \dfrac{G_{\ell_j \ell_i}}{G_{\ell_i}}$ and $\delta_i = \dfrac{N_0}{G_{\ell_i}}$, the second condition could be written using the following matrix form:

$$\underbrace{\begin{pmatrix} P_1 \\ P_2 \\ \ldots \\ P_z \end{pmatrix}}_{\mathcal{P}} \geq \underbrace{\begin{pmatrix} \beta_1 & 0 & \ldots & 0 \\ 0 & \beta_2 & \ldots & 0 \\ \vdots & \vdots & & \vdots \\ 0 & 0 & \ldots & \beta_z \end{pmatrix}}_{\mathcal{B}} \times$$

$$\left(\underbrace{\begin{pmatrix} 0 & \psi_{12} & \ldots & \psi_{1z} \\ \psi_{21} & 0 & \ldots & \psi_{2z} \\ \vdots & \vdots & & \vdots \\ \psi_{z1} & \psi_{z2} & \ldots & 0 \end{pmatrix}}_{\Psi} \underbrace{\begin{pmatrix} P_1 \\ P_2 \\ \ldots \\ P_z \end{pmatrix}}_{\mathcal{P}} + \underbrace{\begin{pmatrix} \delta_1 \\ \delta_2 \\ \ldots \\ \delta_z \end{pmatrix}}_{\Delta} \right) \tag{32}$$

or

$$(I - \mathcal{B}\Psi)\mathcal{P} \geq \mathcal{B}\Delta \tag{33}$$

where I is the $z \times z$ identity matrix.

Defining $\mathcal{A} = \mathcal{B}\Psi$, the necessary and sufficient condition for (33) to have a positive solution $\mathcal{P}$ for every positive vector $\mathcal{B}\Delta$ is that $(I - \mathcal{A})^{-1}$ be nonnegative for $\mathcal{A} \geq 0$. However, for any $\mathcal{A} \geq 0$,

$$(I - \mathcal{A})^{-1} \geq 0 \quad \text{iff} \quad \rho(\mathcal{A}) < 1 \tag{34}$$

where $\rho(\mathcal{A})$ denotes the largest real eigenvalue, also called Perron–Frobenius eigenvalue or spectral radius of matrix $\mathcal{A}$. According to Perron–Frobenius Theorem [33], $\rho(\mathcal{A})$ is positive, and the corresponding eigenvector is positive componentwise.

In addition, considering that the transmission power of each node is upper bounded by P_K, the necessary and sufficient conditions for the existence of a positive $\mathcal{P}^*$ satisfying the SINR constraints in (2) are

$$\rho(\mathcal{B}\Psi) < 1 \quad \text{and} \quad \mathcal{P}^* \preceq \mathcal{P}^{max} \tag{35}$$

where $\mathcal{P}^* = (I - \mathcal{B}\Psi)^{-1}\mathcal{B}\Delta$ and $\mathcal{P}^{max} = (P_K, P_K, \ldots, P_K)$. Note also that $\mathcal{P}^*$ is the componentwise minimum solution of (33).

Of particular interest to us, two links ℓ_i and ℓ_j could be scheduled concurrently if and only if the following conditions are satisfied:

$$\sqrt{\beta_i \beta_j \psi_{ij} \psi_{ji}} < 1 \tag{36}$$

$$\frac{\beta_i(\delta_i + \beta_j \psi_{ij} \delta_j)}{1 - \beta_i \beta_j \psi_{ij} \psi_{ji}} \leq P_K \tag{37}$$

$$\frac{\beta_j(\delta_j + \beta_i \psi_{ji} \delta_i)}{1 - \beta_i \beta_j \psi_{ij} \psi_{ji}} \leq P_K \tag{38}$$

6.2. Valid matching generation algorithm

We describe in the following a heuristic algorithm to find a new matching having a negative reduced-cost to be added as a new column to the RMP in Section 4.1. The main difference with the ILP formulation is that this algorithm terminates as soon as a valid matching is found, not necessarily optimal, although it tries at the same time to find the one with the highest weight.

The cornerstone of this algorithm is the concept of *pairwise link conflict graph* (PLCG). Let $\mathcal{V} = \{(\ell_i, \gamma_{ij}) | \ell_i \in E, \gamma_{ij} \in \{\theta_1, \theta_2, \ldots, \theta_R\}\}$ be a set where each link in E is replicated to form a pair with each data rate satisfying condition (1). We define a PLCG as an undirected graph $\mathcal{G} = (\mathcal{V}, \mathcal{E})$ where there exists an edge between two vertices $v = (\ell, \gamma)$ and $v\prime = (\ell', \gamma\prime)$ if one of the following conditions holds:

- $\ell = \ell'$.
- ℓ and ℓ' are adjacent (share an endpoint).
- One of the conditions (36), (37), or (38) is not satisfied, where β and β' are the minimal SINR thresholds required for γ and $\gamma\prime$, respectively.

The first step is to derive a candidate matching by admitting continuous power levels in $(0, P_K]$. As described in Algorithm 1. We start by building a PLCG graph formed exclusively by the links in E that have a positive dual for the corresponding constraint (8). Then, we create a list $\mathcal{T}$ containing all the vertices in $\mathcal{V}$ sorted by the decreasing order of their weight. Our intention here is to consider first the link/data rate pairs that can decrease the reduced cost by a significant amount. Next, we define a candidate matching m constituted of all the pairs in $\mathcal{T}$ excluding those that form an edge in the PLCG with a prior member of the list or that have been already considered. At this point,

Algorithm 1: *Valid matching generation with continuous power*

input : a set of transmission links/data rates $\mathcal{V} = \{(\ell_1, \gamma_1), (\ell_2, \gamma_2), \ldots, (\ell_n, \gamma_n)\}$ and corresponding positive weights $\{w_1, w_2, \ldots, w_n\}$
output: a matching $m \subseteq \mathcal{V}$ with an associated continuous power vector $\mathcal{P}^{cont}$

build a PLCG graph $\mathcal{G} = (\mathcal{V}, \mathcal{E})$;
$m \leftarrow [\,]$, $\mathcal{T} \leftarrow$ list of elements of $\mathcal{V}$ sorted in the $\searrow$ order of $w_i \gamma_i$;
mark all the elements in $\mathcal{T}$ as .NONVISITED.;
weight $\leftarrow 0$, $j \leftarrow 0$;
while $|\mathcal{T}| > 0$ **do**
  for *i from j+1 to* $|\mathcal{T}|$ **do**
    if *(*$\mathcal{T}[i]$ *is marked as* .NONVISITED.*)* **and** *(*$\forall t \in m, (t, \mathcal{T}[i]) \notin \mathcal{E}$*)* **then**
      $m.add(\mathcal{T}[i])$;
      weight $\leftarrow$ weight $+ w_{\mathcal{T}[i]} \gamma_{\mathcal{T}[i]}$;
    end
  end
  if *weight* > 1 **and** *m is feasible by (35)* **then**
    return m and $\mathcal{P}^{cont}$ calculated by (35);
  else
    if $|m| > 1$ **then**
      $j \leftarrow$ index in $\mathcal{T}$ of the last element of m;
      $m.remove(\mathcal{T}[j])$, $\mathcal{T}[j] \leftarrow$ .VISITED.;
      weight $\leftarrow$ weight $- w_{\mathcal{T}[j]} \gamma_{\mathcal{T}[j]}$;
    else
      $\mathcal{T}.remove(m[1])$, $m.removeall()$;
      mark all the elements in $\mathcal{T}$ as .NONVISITED.;
      weight $\leftarrow 0$, $j \leftarrow 0$;
    end
  end
end
return [ ] *No valid matching has been found*;

if m is a valid matching, the algorithm terminates by returning m and the corresponding power vector. Otherwise, we distinguish two cases:

(1) If m contains more than one element, we remove the last one t, which has also the least weight. Unless m becomes empty, t will not be reconsidered again. Now, we try to add to m all the previously excluded elements that have an edge with t in the PLCG. The resulted matching is checked again, and the procedure repeats.
(2) If m contains only one element, this one is completely removed from $\mathcal{T}$, and the algorithm restarts from the beginning. If $\mathcal{T}$ becomes empty and no valid matching has been found yet, the algorithm terminates with a failure.

If a valid candidate matching with continuous power vector is obtained, the second step, shown in Algorithm 2, is to discretize this vector according to the predefined power levels $P_1, P_2, \ldots, P_K$. Each continuous power in the initial vector, corresponding to some link/data rate pair, is rounded up to the immediate upper P_i ($1 \leq i \leq K$). This relies on the fact that the computed continuous power vector is the componentwise minimum solution to schedulability inequalities as stated previously. The resulting vector would be the final solution if it constitutes a feasible matching. Otherwise, the power of each link whose SINR is below the required threshold is increased to the next P_i, and the matching is checked again. If at some point, the power of a given link is required to be larger than P_K, the algorithm terminates by rejecting the candidate matching. Then, a second valid matching has to come through Algorithm 1 and so on.

Algorithm 2: *Valid matching generation with discrete power*

input : A matching m and a continuous power vector $\mathcal{P}^{cont}$
output: A discrete power vector $\mathcal{P}^{disc}$

for *each* $(\ell, \gamma) \in m$ **do**
  increase p_ℓ to the immediate upper $P_i \in \{P_1, P_2, \ldots, P_K\}$;
end
if $\forall (\ell, \gamma) \in m$, $\text{SINR}_\ell \geq \beta_\gamma$ **then**
  return a vector $\mathcal{P}^{disc}$ containing the discrete power of each element in m. ;
else
  while *true* **do**
    for *each element* $(\ell, \gamma) \in m$, $\text{SINR}_\ell < \beta_\gamma$ **do**
      if $p_\ell = P_K$ **then**
        return [ ]
      end
      increase p_ℓ to the immediate upper $P_i \in \{P_1, P_2, \ldots, P_K\}$;
    end
    recalculate SINR_ℓ for each $(\ell, \gamma) \in m$;
    if $\forall (\ell, \gamma) \in m$, $\text{SINR}_\ell \geq \beta_\gamma$ **then**
      return a vector $\mathcal{P}^{disc}$ containing the discrete power of each element in m. ;
    end
  end
end

As shown in Appendix A, the complexity of Algorithms 1 and 2 is $O(|E|^5 R^2)$ and $O(|E| K)$, respectively. Fortunately, the practical average-case complexity of Algorithm 1 is much more less than that. As described before, it takes as an input only the links that have positive weights (duals) and terminates as soon as a valid matching is found. Moreover, the PLCG graph prevents from including two mutually exclusive links in the same matching.

7. NUMERICAL RESULTS

We discuss in this section the numerical results obtained on the throughput and lifetime maximization problems in various scenarios. We consider network topologies where sensors and targets are deployed on an area measuring 400×400 m^2. Assuming sensors equipped with CC2420 radio transceivers operating in the 2.4 GHz band, eight transmit power levels are programmable [30], namely, $-25, -15, -10, -7, -5, -3, -1$, and 0 dBm. The thermal noise power N_0 is fixed to -40 dBm. The path gain G_{ij} is set to d_{ij}^{-2}, which corresponds to the free space model. Relying on the MCSs proposed in [34] and [35] as an extension to the 802.15.4 standard, the available data rates are {250 kbps, 500 kbps, 1 Mbps, and 2 Mbps} and require the SINR thresholds $\{2, 4, 8$, and $16\}$ in the order. Besides, the sensing range is assumed to be 100 m, and sensors generate a 125-B data packet each time they monitor an associated target.

7.1. Computational results

The mathematical programming models are implemented and solved using CPLEX 12.4 (IBM, Armonk, NY, USA). The experiments are executed on a platform with two Intel 2.93-GHz Xeon X5670 processors (Intel, Santa Clara, CA, USA). Our first investigations, reported in Table I, focus on comparing the cost and the quality of the solutions of the TMP obtained with the ILP versus the heuristic pricing, and those obtained assuming a uniform power level of 0 dBm. Three scenarios are considered with different number of sensors and targets deployed uniformly on the service area. Each row represents the values averaged over a set of 10 problem instances. As expected, the computation time of the optimal solution with the ILP pricing grows exponentially as the number of activable links increases. The uniform power case is less time-consuming than the discrete one because the power variables are eliminated from the pricing. A noticeable result is shown in the "integrality gap" column where the gap between the obtained and the lower bound integer solutions, denoted as Z^* and

Table I. Computational results.

Sensors	Targets	Links	Pricing	Power	CPU time (s)	Number of iterations	Integrality gap (%)	Gap with *E/D* (%)	Links/ matching	Cap./matching (kbps)
			Exact	Disc.	783	87	0.01	—	2.00	714
30	75	42	Heuri.	Disc.	5	90	0.07	2.51	1.97	728
			Exact	Unif.	326	82	0.75	2.58	1.95	744
			Exact	Disc.	6479	184	0.01	—	2.37	932
40	150	72	Heuri.	Disc.	36	173	0.01	2.50	2.14	971
			Exact	Unif.	2904	185	0.42	4.97	2.34	1121
			Exact	Disc.	27 149	285	0.01	—	2.45	1031
50	200	104	Heuri.	Disc.	149	269	0.03	1.91	2.23	1131
			Exact	Unif.	12 250	293	0.39	4.59	2.35	1181

CPU, central processing unit; Disc., discrete; Unif., uniform; Cap., capacity; Heuri., heuristic.

Z^{ILP} in Section 4.2, respectively, does not exceed 1% in all the cases. Hence, the optimal solution of the TMP is achieved in most cases.

Furthermore, the heuristic pricing provides a set of matchings that leads to solutions within 3% of optimality with the considerable benefice of much less computation time. This is mainly due to the ability of Algorithms 1 and 2 to find the matchings with the link/data rate pairs that have a high impact on reducing the TDMA frame length. Also, a link ℓ that is disabled in Algorithm 1 (i.e., marked as visited) may be reconsidered again if the interfering links, identified by the incident edges of ℓ in the PLCG, have been removed. Hence, this algorithm can span a wide region of the search space. Another good accuracy indicator is provided by the number of CG iterations. Here, we see that the number of times the heuristic approach succeeds to find a new matching is very close to the exact method. Also, the short running time of the heuristic approach could be explained first by the fact that we do not add to the matching any link that causes pairwise interference with existing links. This reduces significantly the size of the matrices involved in the feasibility check (35). Also, the Algorithm (1) behaves greedily at some point as each link removed from the list (line 20) will not be reconsidered again.

In general, the exact ILP discrete pricing produces matchings containing slightly more links, but it remains below our heuristic pricing in terms of capacity. Also, although the matchings used to build the uniform power solution may include more links and reach higher capacities, they do not necessarily yield the shortest TDMA frame. Indeed, many matchings that are able to gather "critical" links are only feasible with varying power levels.

7.2. Throughput evaluation

We examine in this section how the network throughput evolves as a function of the number of targets, the number of sensors, or the coverage level. Note that we refer here to the throughput as the amount of traffic that reaches the sink per time unit. In a first set of experiments, we deploy 40 sensors over the area and a variable number of targets ranging from 40 to 220. For comparison purposes, we run also a single-rate strategy with the standardized 250 kbps data rate. We observe in Figure 1 the relative stability of network throughput. This is due to the TDMA access scheme preventing network collapse even when the traffic intensity increases, unlike random access schemes such as Carrier Sense Multiple Access (CSMA). Besides, multiple-rate strategies clearly outperform single-rate ones by at

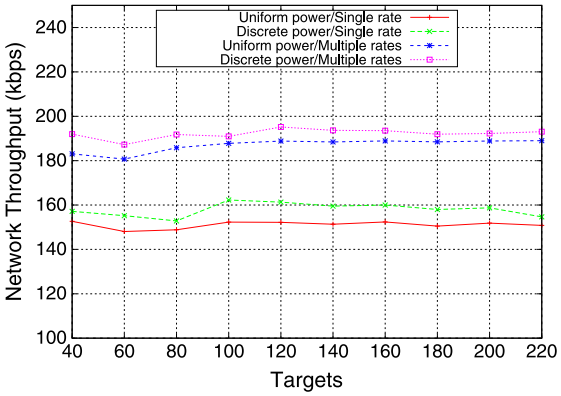

Figure 1. Network throughput (40 sensors).

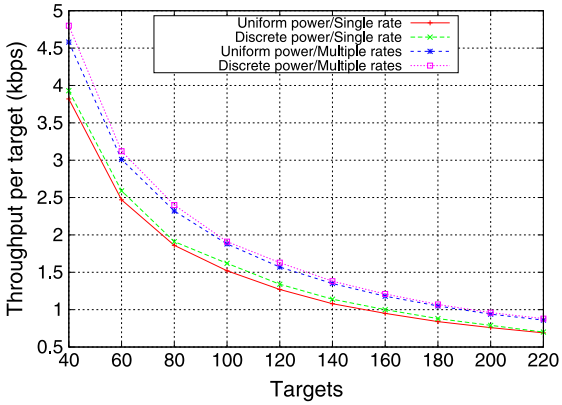

Figure 2. Throughput per target (40 sensors).

least 20%. Also, discrete power enhances consistently the throughput compared to uniform power. However, individual targets would be less monitored per time unit in both cases as their number increases. The average throughput per target, depicted in Figure 2, seems to follow a logarithmic decrease for each tested strategy.

The experiment reported in Figure 3 illustrates the effect of sensor density on throughput. Assuming 150 uniformly deployed targets, the network scenario is solved by first deploying 40 sensors covering all the targets and then gradually increasing their number. One would remark the quasi-linear increase of throughput per target as a function of the number of sensors using each of the four strategies. The benefit of using multiple rates is even more substantial as the number of sensor increases. These results suggest that WSNs formed by many low-range and high-rate transmission links result in much higher throughput than the ones with fewer long-range and low-rate transmission links.

Next, we illustrate in Figure 4 the impact of coverage level on throughput. By solving two problem instances, ($n = 40$, $h = 80$) and ($n = 50$, $h = 150$), where the coverage level q varies between 1 and 4, we observe that the throughput per target decreases linearly when q increases.

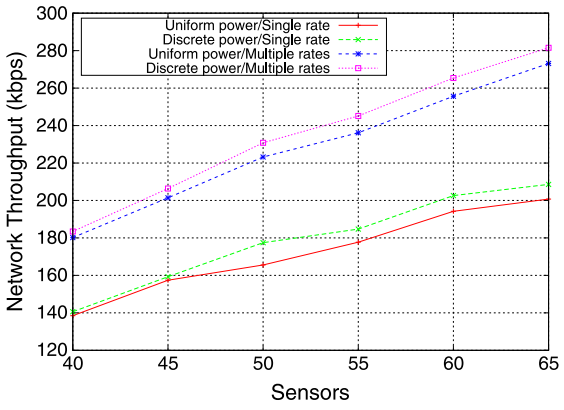

Figure 3. Throughput (150 targets).

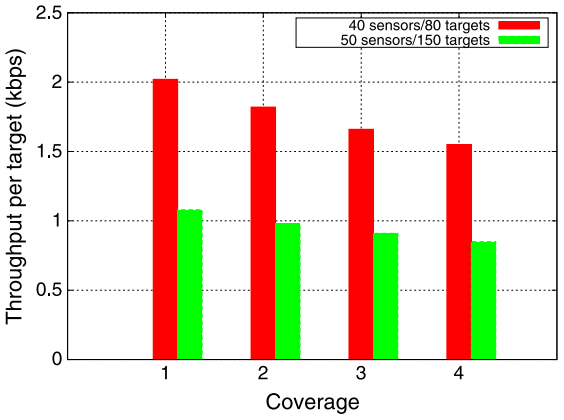

Figure 4. Throughput versus coverage level.

Regardless on reliability requirements that may impose to monitor each target by multiple sensors, these results suggest that more data about a given target are delivered to the sink per time unit when this one is monitored by a single sensor rather than by several ones. This means that there exists a tradeoff to consider between throughput and sensing reliability when it comes to specify the number of sensors monitoring each target.

7.3. Evaluation of throughput-lifetime tradeoff

We report in this section the results obtained by solving the lifetime maximization problem in various settings. First, note that the CC2420 radio transceiver [30] associates a current draw (in mA) to each output power. According to the programmable transmit powers P_k ($1 \leq k \leq 8$), the set of corresponding currents are $\{8.5, 9.9, 11.2, 12.5, 13.9, 15.2, 16.5, 17.4\}$. Consequently, the consumption power P_k^{tx} at each level is calculated by the product of the corresponding current consumption and the supply voltage 1.8 V. In case of receive state, the needed current consumption is 19.7 mA. This results in higher energy consumption that transmit state. This fact contrasts with the assumption made in several works on the higher incurred energy cost of transmission [36]. On the other hand, the sensing energy can vary considerably depending on the sensor characteristics and the observed phenomenon. For evaluation purposes, we fix the energy e_{max}^s consumed by a sensor to monitor a target situated at the maximal distance to five times the energy spent to transmit a data packet of 125 B with the maximal power P_K and the lowest rate θ_1. The reason is to boost the impact of sensor-target associations on the solutions considering that radio transmissions consume anyway more energy during the TDMA frame.

Figures 5a and 5b show an illustrative example on the resulting traffic paths (represented with solid arrows) and the sensor-target associations (represented with dotted arrows), where two different lengths of the TDMA frame are considered: 135 and 250 ms. The WSN is formed by a grid of 36 sensors and 30 uniformly deployed targets, depicted by green and yellow disks, respectively. The blue disk corresponds to the sink. Each target is monitored by two sensors. In Figure 5, where the TDMA frame has the minimum length, we observe that the four closest sensors to the sink are used intensively both for sensing and relaying. By taking advantage of the low-range transmissions of these sensors, other links can be scheduled concurrently. Also, many data packets are just one hop away from the sink, which contributes to decrease the TDMA cycle. In Figure 5, we notice that there are other sensors that transmit directly their data to the sink and that some targets are now associated with remote sensors. In sum, if the maximum length of the frame is raised by a factor of 1.8, the network lifetime, expressed as the number of TDMA cycles, is raised by a factor of 3.3. However, the drawback will be less throughput and higher end-to-end delays.

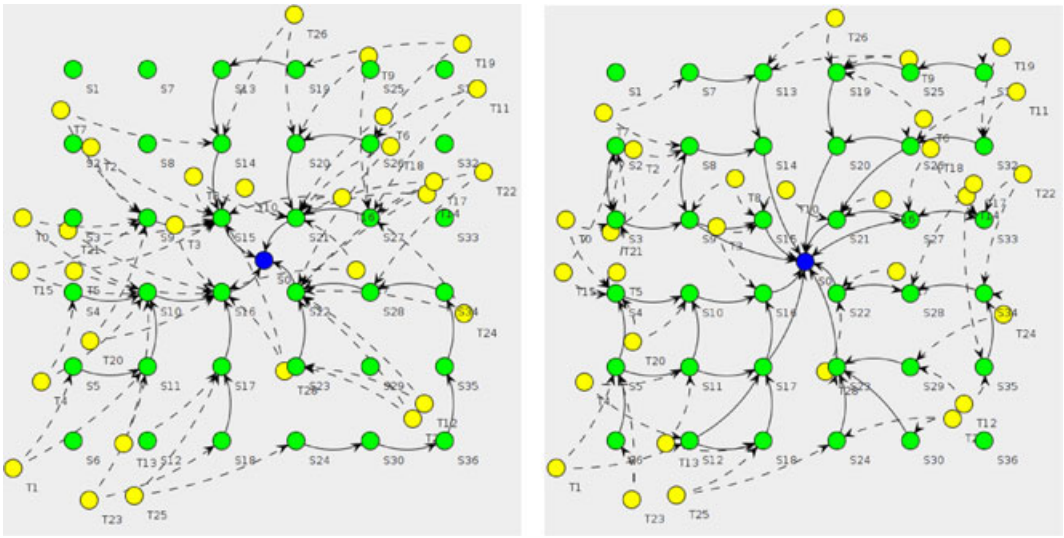

(a) 135ms **(b)** 250ms

Figure 5. Solutions of a network scenario with different time division multiple access (TDMA) frame lengths.

Similarly, this throughput-lifetime tradeoff appears in another network scenario, where 49 sensors are disposed on a grid and 200 targets are deployed uniformly. Figure 6 presents the network lifetime as a function of the length of the TDMA frame, by considering both discrete and uniform power strategies. We assume here that the initial energy at each sensor is 64 800 J corresponding to two standard AAA batteries. Note that each considered TDMA length may contain an idle portion where no transmissions are scheduled. That is, this prescribed length, denoted as T_{frame} in the lifetime-RMP formulation, may be strictly greater than the TDMA length actually calculated in the solution. We observe that the lifetime in both cases increases almost linearly, starting with the minimum possible lengths, which are derived by solving the TMP problem. However, a significant gap of about 20% exists between the two strategies for applicable frame lengths. Moreover, only discrete strategy is feasible where the TDMA frame length is below 1200 ms. Likewise, Figure 7 depicts the number of achievable TDMA cycles with both strategies by normalizing the initial energy to 1 J. This number gives a measure on how many target monitorings will be gathered during the network lifetime. We observe that it reaches a limit when the TDMA frame exceeds a certain length. The discrete power strategy outperforms clearly the uniform one, but the gap between the two decreases as the TDMA length increases.

Figure 8 shows a discrete power scenario with 100 targets where the number of achievable TDMA cycles is given for a number of sensors ranging from 35 to 55. Clearly, a huge improvement of lifetime is made for a given TDMA frame length when the network is formed by more sensors. For example, if the TDMA frame length is bounded by 400 ms, the lifetime increases from 120 cycles with 35 sensors to 440 cycles with 55 sensors. However, the maximal

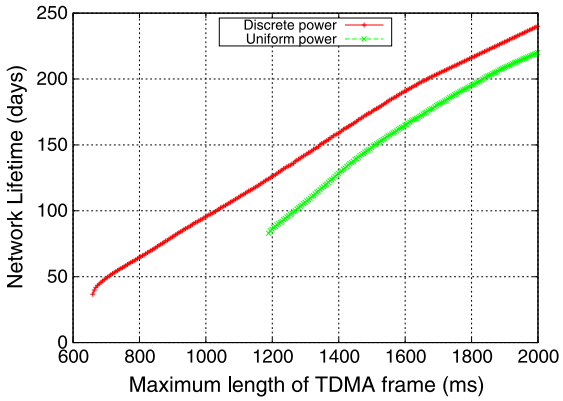

Figure 6. Network lifetime (49 sensors, 200 targets).

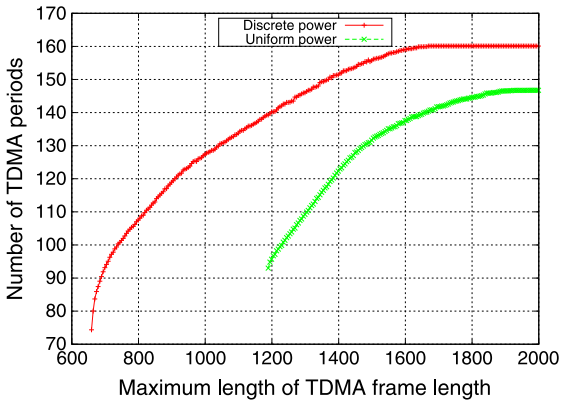

Figure 7. Time division multiple access (TDMA) cycles (49 sensors, 200 targets).

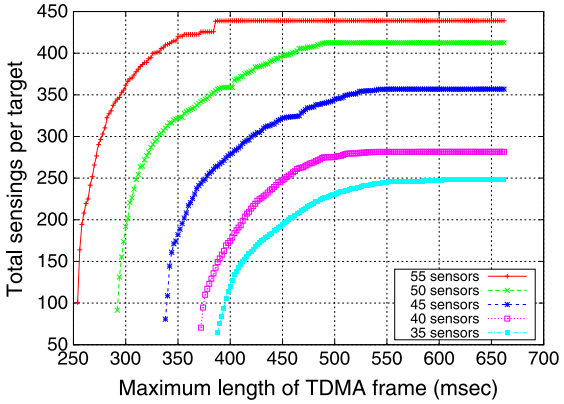

Figure 8. Time division multiple access (TDMA) cycles (100 targets).

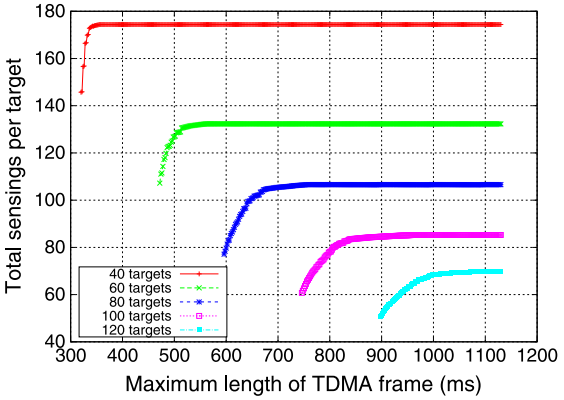

Figure 9. Time division multiple access (TDMA) cycles (40 sensors).

gap will be just about 75% when the TDMA frame is large. This suggests that depending on the desired network lifetime and throughput, one has to deploy a sufficient number of sensors.

Finally, Figure 9 represents the converse case where the number of targets augments, whereas the number of sensors remains fixed. By adding 20 targets at each step, starting from 40, we remark that lifetime reduction is fast at the beginning (25%) but gradually falls below 15%. Hence, the lifetime is more sensitive to the increase factor than to the number of targets actually added. Interestingly, the convergence of the number of TDMA cycles is very fast with lightweight traffic demands, which means that the lifetime can be extended significantly at a moderate cost in terms of throughput and delay. In contrast, the increase is slower with heavy traffic demands, which implies that a wider range of lifetime-throughput combinations is attractive depending on application requirements.

7.4. Comparison with previous works

Fu *et al.* addressed in [12] a joint power control and scheduling problem in TDMA wireless networks using a CG approach, where the optimal solutions are obtained through a branch-and-price method. Although the overall objective is different, the formulated pricing problem is similar to ours. There are however two notable differences as they assume continuous powers and fixed data rates. To solve this problem efficiently, they propose in particular a heuristic algorithm where one link is removed at a time from the initial maximal matching m. The decision on the link to remove depends on which condition is not satisfied in (35). In the first case where the Perron–Frobenius eigenvalue is higher than one, they remove the link that maximizes the row sum and the column sum of the matrix $\mathcal{A}$ (Section 6.1). The second case is addressed by removing the link whose power exceeds the maximum power with the maximum amount. In case where this algorithm fails to find a feasible matching, an exact algorithm called *smart enumeration*, having an exponential complexity, is executed.

By contrast, our approach to solve the pricing problem is based on a different manner to walk through the list of links and eliminates from matrix calculations many links thanks to the PLCG graph. This has a considerable impact on computation times. As a comparison, the results in [12] report that the average runtime for a network with 32 links is 269 s, while our approach is able to solve instances with 104 links in just 149 s (Table I). Note that 104 links in our case correspond actually to possibly 416 links in case of [12] because we may replicate each link multiple times according to the number of possible data rates. Additionally, even though our solutions are not always optimal as in [12], the achieved accuracy is consistently high.

On another hand, our results about optimal lifetime versus throughput requirements can be thought as a generalization of some results observed by Luo *et al.* in [26]. Assuming fixed transmission power and MCS, they suggested that there is a threshold level in the throughput requirement below which reduction of the throughput requirement results in only a proportional improvement in lifetime. But above that threshold, lifetime can improve much better than proportionally. The same behavior can be easily observed in our results using variables transmission powers and MCSs. For example, in Figure 6, the network lifetime increase is linear to the decrease of the throughput. Whereas, Figures 8 and 9 exhibit a throughput threshold where lifetime falls dramatically if it is exceeded.

8. CONCLUSION

We studied in this paper the optimal TDMA link scheduling in WSNs. We designed a set of optimization models to derive schedules that either maximize network throughput or maximize network lifetime subject to a required minimum throughput. By leveraging advanced networking capabilities offered by current sensors, a wide

range of network parameters are considered in the solution related to coverage, routing, power control, and rate adaptation. Because the straightforward ILP formulations of theses problems are NP-hard, we introduced a computationally feasible column-generation-based method to compute near-optimal solutions when the RMP is formulated as an ILP. Furthermore, because the underlying pricing problem remains also NP-hard, we proposed a polynomial-time heuristic algorithm that searches for valid matchings composed by a set of power-controlled concurrent links with prescribed data rates. Besides, our energy consumption model is based on a real-world hardware platform, hence providing accurate measures of transmit and receive energy costs.

Our numerous experimentations shed the light on several outcomes. First, our heuristic algorithm showed its efficiency even when the number of activable links increases. As expected, power control and rate adaptation improve the overall throughput and lifetime by a comfortable margin. Furthermore, sensor density is found to have a major impact on performance, whereas Q-coverage induces a tradeoff between throughput and monitoring reliability. Another noticeable result is that heavy traffic demands cause a wide range of relevant throughput-lifetime tradeoffs depending on application requirements, while lightweight demands can be managed efficiently without much sacrifice on one side or the other.

APPENDIX A. COMPLEXITY OF ALGORITHMS 1 AND 2

It can be seen in Algorithm 1 that the list $\mathcal{T}$ contains initially at most $|E| \times R$ elements that represent all the possible vertices of the pairwise link conflict graph (Section 6.2). In the worst case, each element is ultimately removed from the list through line 20. At each iteration of the outer loop (lines 5–25), the elements of $\mathcal{T}$ represent no more than $i \leq |E|$ distinct links. The inner loop (lines 6–11) tries at each iteration to add another link to the candidate matching m. Hence, knowing that each link can be associated to R different rates, at most, $\sum_{j=1}^{i-1} Rcj^3$ operations are executed before an element is removed. The term cj^3, where c is a positive constant, corresponds to the supposed cost of the calculations of the eigenvalue and the inverse of a matrix having the same order j as the number of current links in m. Recall that any matching cannot contain the same link with different rates. At the end, a total of $R^2 c \sum_{i=1}^{|E|} \sum_{j=1}^{i-1} j^3$ is executed. Hence, the complexity of Algorithm 1 is $O(|E|^5 R^2)$.

The complexity of Algorithm 2 is easy to derive because in the worst case, we check the discrete power combinations over all the links, which gives $O(|E| K)$.

REFERENCES

1. Hunkeler U, Lombriser C, Truong HL, Weiss B. A case for centrally controlled wireless sensor networks. *Computer Networks* 2013; **57**(6): 1425 –1442.
2. Zinonos Z, Vassiliou V, Ioannou C, Koutroullos M. Dynamic topology control for WSNs in critical environments. In *New technologies, mobility and security (NTMS), 2011 4th IFIP international conference on*, 2011; 1–5.
3. Shi Y, Hou YT, Liu J, Kompella S. Bridging the gap between protocol and physical models for wireless networks. *Mobile Computing, IEEE Transactions on* 2013; **12**(7): 1404–1416.
4. ElBatt T., Ephremides A. Joint scheduling and power control for wireless ad hoc networks. *Wireless Communications, IEEE Transactions on* 2004; **3** (1): 74–85.
5. Borbash S, Ephremides A. Wireless link scheduling with power control and SINR constraints. *Information Theory, IEEE Transactions on* 2006; **52**(11): 5106–5111.
6. Tang J, Xue G, Chandler C, Zhang W. Link scheduling with power control for throughput enhancement in multihop wireless networks. *Vehicular Technology, IEEE Transactions on* 2006; **55**(3): 733–742.
7. Fu L, Liew SC, Huang J. Joint power control and link scheduling in wireless networks for throughput optimization. In *Communications, 2008. ICC '08. IEEE international conference on*, 2008; 3066–3072.
8. Grandhi S, Vijayan R, Goodman D, Zander J. Centralized power control in cellular radio systems. *Vehicular Technology, IEEE Transactions on* 1993; **42**(4): 466–468.
9. Kim W, Park JS. Cross-layer scheduling for multi-users in cognitive multi-radio mesh networks. *Wireless Communications and Mobile Computing* 2014; **14**(11): 1034–1044.
10. Djukic P, Valaee S. Delay aware link scheduling for multi-hop TDMA wireless networks. *Networking, IEEE/ACM Transactions on* 2009; **17**(3): 870–883.
11. Wang Q, Wu DO, Fan P. Delay-constrained optimal link scheduling in wireless sensor networks. *Vehicular Technology, IEEE Transactions on* 2010; **59**(9): 4564–4577.
12. Fu L, Liew SC, Huang J. Fast algorithms for joint power control and scheduling in wireless networks. *Wireless Communications, IEEE Transactions on* 2010; **9**(3): 1186–1197.
13. Ergen SC, Varaiya P. TDMA scheduling algorithms for wireless sensor networks. *Wireless Networks* 2010-05; **16**(4): 985–997.

14. Hedayati K, Rubin I, Behzad A. Integrated power controlled rate adaptation and medium access control in wireless mesh networks. *Wireless Communications, IEEE Transactions on* 2010; **9**(7): 2362–2370.
15. Kompella S, Wieselthier JE, Ephremides A, Sherali HD, Nguyen GD. On optimal SINR-based scheduling in multihop wireless networks. *IEEE/ACM Trans. Netw.* 2010-12; **18**(6): 1713–1724.
16. Dai X, Omiyi PE, Br K, Yang Y. Interference-aware convergecast scheduling in wireless sensor/actuator networks for active airflow control applications. *Wireless Communications and Mobile Computing* 2014; **14**(3): 396–408.
17. Madan R, Cui S, Lall S, Goldsmith A. Modeling and optimization of transmission schemes in energy-constrained wireless sensor networks. *Networking, IEEE/ACM Transactions on* 2007; **15**(6): 1359–1372.
18. Wang H, Yang Y, Ma M, He J, Wang X. Network lifetime maximization with cross-layer design in wireless sensor networks. *Wireless Communications, IEEE Transactions on* 2008; **7**(10): 3759–3768.
19. Cardei M, Thai MT, Li Y, Wu W. Energy-efficient target coverage in wireless sensor networks. In *INFOCOM 2005. 24th annual joint conference of the ieee computer and communications societies. proceedings ieee*, 2005; 1976–1984 vol. 3.
20. Gu Y, Li J, Zhao B, Ji Y. Target coverage problem in wireless sensor networks: a column generation based approach. In *Mobile adhoc and sensor systems, 2009. MASS '09. IEEE 6th international conference on*, 2009; 486–495.
21. Pyun SY, Cho DH. Energy-efficient scheduling for multiple-target coverage in wireless sensor networks. In *Vehicular technology conference (VTC 2010-spring), 2010 ieee 71st*, 2010; 1–5.
22. Turkogullari YB, Aras N, AltÄśnel ÄŕK, Ersoy C. A column generation based heuristic for sensor placement, activity scheduling and data routing in wireless sensor networks. *European Journal of Operational Research* 2010; **207**(2): 1014 –1026.
23. Rossi A, Singh A, Sevaux M. An exact approach for maximizing the lifetime of sensor networks with adjustable sensing ranges. *Computers and Operations Research* 2012; **39**(12): 3166 –3176.
24. Zhu J, Chen S, Bensaou B, Hung KL. Tradeoff between lifetime and rate allocation in wireless sensor networks: a cross layer approach. In *INFOCOM 2007. 26th IEEE International Conference on Computer Communications. IEEE*, 2007; 267–275.
25. Quintas D, Friderikos V. Energy efficient spatial TDMA scheduling in wireless networks. *Computers and Operation Research* 2012-09; **39**(9): 2091–2099.
26. Luo J, Iyer A, Rosenberg C. Throughput-lifetime trade-offs in multihop wireless networks under an SINR-based interference model. *Mobile Computing, IEEE Transactions on* 2011; **10**(3): 419–433.
27. Goussevskaia O, Pignolet YA, Wattenhofer R. Efficiency of wireless networks: approximation algorithms for the physical interference model. *Found. Trends Netw.* 2010-03; **4**(3): 313–420.
28. Uddin MF, Assi C. Joint routing and scheduling in WMNs with variable-width spectrum allocation. *IEEE Transactions on Mobile Computing* 2013; **12**(11): 2178–2192.
29. Cormen TH, Stein C, Rivest RL, Leiserson CE. *Introduction to Algorithms* (2nd edn). McGraw-Hill Higher Education, 2001.
30. *Chipcon CC2420 datasheet: http://focus.ti.com/lit/ds/symlink/cc2420.pdf, Texas Instruments*, 2007.
31. Goussevskaia O, Oswald YA, Wattenhofer R. Complexity in geometric SINR. In *Proceedings of the 8th ACM International Symposium on Mobile Ad Hoc Networking and Computing, MobiHoc '07,* ACM: New York, NY, USA, 2007; 100–109.
32. Bambos N, Chen S, Pottie G. Channel access algorithms with active link protection for wireless communication networks with power control. *Networking, IEEE/ACM Transactions on* 2000; **8**(5): 583–597.
33. Pillai SU, Suel T, Cha S. The Perron-Frobenius theorem: some of its applications. *Signal Processing Magazine, IEEE* 2005; **22**(2): 62–75.
34. Skyworks. Extending 2.4 GHz Zigbee short-range radio performance with skyworks sky65336/sky65337 front-end modules, 2011.
35. Lanzisera S, Mehta AM, Pister KSJ. Reducing average power in wireless sensor networks through data rate adaptation. In *Proceedings of the 2009 IEEE international conference on communications, ICC'09*. IEEE Press, Piscataway, NJ, USA, 2009; 480–485.
36. Chen B, Jamieson K, Balakrishnan H, Morris R. Span: an energy-efficient coordination algorithm for topology maintenance in ad hoc wireless networks. *Wireless Networks* 2002-09; **8**(5): 481–494.

AUTHORS' BIOGRAPHY

Mejdi Kaddour received the Engineer and the MS degrees in Computer Science from the University of USTO-MB, Oran, Algeria, in 1997, and the University of Pierre and Marie Curie, Paris, France, in 2001, respectively. Then, he received the PhD degree in Computer Science and Networking from Télécom ParisTech, France, in 2005. He worked from 2005 to 2006 as a postdoctoral fellow at Télécom SudParis, Evry, France. He joined the University of Oran 1, Algeria, in 2007, where he currently holds an associate professor position. He is also the leader of the Algorithms and Optimization for Communication Networks team of the LITIO Laboratory at the same University. His research interests focus on the design of efficient cross-layer optimization methods and algorithms for wireless sensor networks, wireless mesh networks, and cognitive radio networks. He is also working on performance evaluation and quality of service in communication networks.